2

Biochemical Analysis of Halophilic Dehydrogenases Altered by Site-Directed Mutagenesis

J. Esclapez, M. Camacho, C. Pire and M.J. Bonete
Departamento de Agroquímica y Bioquímica, División de Bioquímica y Biología Molecular, Facultad de Ciencias, Universidad de Alicante, Alicante, Spain

1. Introduction

Extremely halophilic Archaea are found in highly saline environments such as natural salt lakes, saltern pools, the Dead Sea and so on. These microorganisms require between 2.5 and 5.2 M NaCl for optimal growth. They can balance the external concentration by accumulating intracellular KCl to concentrations that can reach and exceed saturation. The biochemical machinery of these microorganisms has, therefore, been adapted in the course of evolution to be able to function at salt concentrations at which most biochemical systems will cease to function. The biochemical and biophysical properties of several halophilic enzymes have been studied in great detail; and, as a general rule, it was found that the halophilic enzymes are stabilized by multimolar concentration of salts. In most cases the salt also stimulates the catalytic activity. This stabilization of halophilic proteins in solvents containing high salt concentrations has been discussed in terms of apparent peculiarities in their composition. Since the first amino acid composition determinations, it has become clear that halophilic enzymes present a higher proportion of acidic over basic residues, an increase in small hydrophobic residues, a decrease in aliphatic residues and lower lysine content than their non-halophilic homologues (Lanyi, 1974; Eisenberg, et al., 1992; Madern et al., 2000). Since then, structural analyses have revealed two significant differences in the characteristics of the surface of the halophilic enzymes that may contribute to their stability in high salt. The first of these is that the excess of acidic residues are predominantly located on the enzyme surface leading to the formation of a hydration shell that protects the enzyme from aggregation in its highly saline environment. The second is that the surface also displays a significant reduction in exposed hydrophobic character, which arises not from a loss of surface exposed hydrophobic residues but from a reduction in surface-exposed lysine residues. Nevertheless, although the number of halophilic protein sequences has increased during the last years, the number of high resolution structures that permit the details of the protein solvent interactions to be seen is limited. The role of the reduction in the surface lysines has been largely ignored (Britton et al., 1998, 2006). Furthermore, in several studies, the authors have concluded that it is the precise structural organization of surface acidic residues that is important in halophilic adaptation. Not only is there an increase in acidic residue content, but these residues form clusters that bind networks of hydrated ions (Richard et al., 2000).

Halophilic archaea are considered a rather homogeneous group of heterotrophic microorganisms predominantly using amino acids as their source of carbon and energy. However, it has been shown that some halophilic archaea are able to use not only amino acids but different metabolites as well, as, for example, *Haloferax mediterranei,* which grows in a minimal medium containing glucose as the only source of carbon using a modified Entner-Doudoroff pathway (Rodriguez-Valera et al., 1983), or *Haloferax volcanii,* which is also able to grow in minimal medium with acetate as the sole carbon source (Kauri et al., 1990). Isocitrate lyase and malate synthase activities were detected in this organism when it was grown on a medium with acetate as the main carbon source (Serrano et al., 1998).

To understand the molecular basis of salt tolerance responsible for halophilic adaptation of proteins, to analyze the coenzyme specificity, and to study the mode of zinc-binding, we have chosen as model enzymes two halophilic dehydrogenase proteins involved in carbon catabolism. They are the glucose dehydrogenase (GlcDH) and isocitrate dehydrogenase (ICDH) from the extremely halophilic Archaea *Haloferax mediterranei* and *Haloferax volcanii*, respectively.

1.1 *Haloferax mediterranei* glucose dehydrogenase

GlcDH is the first enzyme of a non-phosphorylated Entner-Doudoroff pathway. It catalyses the reaction:

$$\text{Glucose} + \text{NAD(P)}^+ \rightarrow \text{Glucono-1,5-lactone} + \text{NAD(P)H} + \text{H}^+$$

GlcDH from *Hfx. mediterranei* has been characterized and purified using gel filtration and affinity chromatography in the presence of buffers containing a high concentration of salt or glycerol to stabilize its structure. The protein is a dimeric enzyme with a molecular weight of 39 kDa per subunit, and shows a dual cofactor specificity, although it displays a marked preference for $NADP^+$ to NAD^+. Biochemical studies have established that the presence of a divalent ion such as Mg^{2+} or Mn^{2+} at concentrations of 25 mM enhances enzymatic activity (Bonete et al., 1996). Inactivation by metal chelators and reactivation by certain divalent ions indicated that glucose dehydrogenase from *Hfx. mediterranei* contains tightly bound metal ions that are essential for activity. Studies on the metal content of the enzyme by ICP revealed the presence of zinc ions whose removal by addition of EDTA leads to complete loss of enzyme activity (Pire et al., 2000). Sequence analysis showed that this enzyme belongs to the zinc-dependent medium-chain alcohol dehydrogenase superfamily (MDR), which includes sorbitol dehydrogenases, xylitol dehydrogenases and alcohol dehydrogenases (Pire et al., 2001). The structure of *Hfx. mediterranei* GlcDH has been solved at the highest resolution to date for any water-soluble halophilic enzyme. The structures of the apoenzyme and a D38C mutant in complex with $NADP^+$ and zinc reveal that the subunit, like that of the other MDR family members, is organized into two domains separated by a deep cleft, with the active site lying at its base. Domain 1 contains the residues involved in substrate binding, catalysis, and coordination of the active-site zinc. Domain 2 consists of a dinucleotide-binding Rossmann fold (Rossmann et al., 1974) that is responsible for binding $NADP^+$. Its molecular surface is predominantly covered by acidic residues, which are only partially neutralized by bound potassium counterions that also appear to play a role in substrate binding. The surface shows the expected reduction in hydrophobic character associated with the loss of lysines, which is consistent with the

genome-wide reduction of this residue in extreme halophiles. The structure also reveals a highly ordered, multilayered solvation shell that can be seen to be organized into one dominant network covering much of the exposed surface accessible area to an extent not seen in almost any other protein structure solved (Ferrer et al., 2001; Britton et al., 2006). Recently, high-resolution structures of a series of binary and ternary complexes of halophilic GlcDH have allowed an extension of the understanding of the catalytic mechanism in the MDR family. In contrast to the textbook MDR mechanism in which the zinc ion is proposed to remain stationary and attached to a common set of protein ligands, analysis of these structures reveals that in each complex, there are dramatic differences in the nature of the zinc ligation. These changes arise as a direct consequence of linked movements of the zinc ion, a zinc-bound bound water molecule, and the substrate during progression through the reaction. These results provide evidence for the molecular basis of proton traffic during catalysis, a structural explanation for pentacoordinate zinc ion intermediates, and a unifying view for the observed patterns of metal ligation in the MDR family (Esclapez et al., 2005; Baker et al., 2009).

1.2 *Haloferax volcanii* isocitrate dehydrogenase

The citric acid cycle enzyme, ICDH (EC 1.1.1.41 and EC 1.1.1.42), catalyses the oxidative decarboxylation of isocitrate (Kay & Weitzman, 1987):

$$\text{Isocitrate} + \text{NAD(P)}^+ \rightarrow \text{2-oxoglutarate} + \text{NAD(P)H} + \text{H}^+ + \text{CO}_2$$

The wild-type enzyme from *Haloferax volcanii* was purified using three steps. The enzyme has been characterized, and it is a dimer with subunit M_r of 62000 Da. Its activity is strictly NADP dependent, and markedly dependent on the concentration of NaCl or KCl, being maximal in 0.5 M NaCl or KCl. The thermostability of the archaeal isocitrate dehydrogenase was investigated incubating the enzyme in buffer containing either 0.5 M or 3 M KCl. Clearly, the thermal stability of the enzyme is substantially reduced at the lower KC1 concentration, with concomitant differences in the activation energies for the thermal inactivation process, 360 kJ mol^{-1} and 610 kJ mol^{-1} at 0.5 M and 3 M KCl, respectively; therefore, the high *in vivo* KC1 concentrations appear to be more important for the stability of the enzyme than for its catalytic ability (Camacho et al., 1995). The gene encoding this protein was sequenced and the derived amino acids were determined. The yields of *Escherichia coli*-expressed enzyme were greater than those obtained by purification of the enzyme from the native organism, but the product was insoluble inclusion bodies. The recombinant ICDH behaves similarly to the native enzyme with respect to the dependence of activity on salt concentration. Kinetic analysis has also shown the purified recombinant and native enzymes to be similar, as are the thermal stabilities (Camacho et al., 2002). *Hfx. volcanii* ICDH dissociation/deactivation has been measured to probe the respective effect of anions and cations on stability. Surprisingly, enzyme stability has been found to be mainly sensitive to cations and very little (or not) to anions. Divalent cations have induced a strong shift of the active/inactive transition towards low salt concentration. A high resistance of ICDH from *Hfx. volcanii* to chemical denaturation has also been found. This study strongly suggests that *Hfx. volcanii* ICDH might be seen as a type of halophilic protein never described before: an oligomeric halophilic protein devoid of intersubunit anion-binding sites (Madern et al., 2004).

2. Materials and methods

2.1 Strains, culture conditions and vectors

Escherichia coli NovaBlue (Novagen) was used as host for plasmids pGEM-11Zf(+) and pET3a. *E. coli* BMH71-18 *mutS* (Promega) and *E. coli* XL1-Blue (Stratagene) were employed in site-directed mutagenesis experiments. *E. coli* BL21(DE3) (Novagen) was used as the expression host. *E. coli* strains were grown in Luria-Bertani medium at 37 ºC with shaking at 180 rpm. Plasmids were selected for in solid and liquid media by the addition of 100 μg ampicillin/ml.

Vector pGEM-11Zf(+) (Promega) was used for cloning genes and carrying out some site-directed mutagenesis experiments. The expression vector pET3a was purchased from Novagen.

2.2 Site-directed mutagenesis

Site-directed mutations were introduced into genes cloned in pGEM-11Zf(+) or directly into pET3a expression vector. The synthetic oligonucleotide primers (Applied Biosystems and Bonsai Technology) were designed to contain the desired mutation. Mutant construction was carried out by two different methods. In the first, the gene encoding the halophilic dehydrogenases were cloned into pGEM-11Zf(+) and site-directed mutagenesis was performed using the GeneEditorTM *in vitro* Site-Directed Mutagenesis System (Promega). This method works by the simultaneous annealing of two oligonucleotide primers to one strand of a denaturated plasmid. One primer introduces the desired mutation in the gene; and the other primer mutates the beta-lactamase gene, increasing the resistance to alternate antibiotics as penicillins and cephalosporines. The last change is important to select plasmids derived from the mutant strand. This positive selection results in consistently high mutagenesis efficiencies. The protocols supplied with the kit consist in the annealing of the two oligonucleotide primers to an alkaline-denatured dsDNA template. Following hybridization, the oligonucleotides are extended with DNA polymerase to create a double-stranded structure. The nicks are then sealed with DNA ligase and the duplex structure is used to transform an *E. coli* host. The construction of the mutants was carried out following the Promega protocol but with one modification: the length of the DNA denaturation stage was increased from 5 min at room temperature to 20 min at 37 ºC due to the increase of the GC content in the halophilic genomes. In the second, the mutagenesis procedure used followed the method of the Stratagene Quick Change kit, using *Pfu Turbo* DNA polymerase from Stratagene. Extension of the oligonucleotide primers generated a mutated plasmid containing staggered nicks. Following temperature cycling, the product was treated with *Dpn* I (Fermentas). The *Dpn* I endonuclease is specific for methylated and hemimethylated DNA and was used to digest the parental DNA template and to select for mutation containing synthesized DNA. The nicked vector DNA containing the desired mutations was transformed into XL1-Blue competent cells (CNB Fermentation Service). In both methods, putative mutants were screened by dideoxynucleotide sequencing with ABI3100 DNA sequencer (Applied Biosystems).

2.3 Protein preparation

Expression *E. coli* BL21(DE3) cells were transformed with the mutated plasmid. Expression, renaturation and purification of recombinant mutants were as previously described for wild

type halophilic enzymes (Pire et al., 2001; Camacho et al., 2002). The purity of the proteins was checked by SDS–polyacrylamide gel electrophoresis (SDS-PAGE). No protein contamination was detectable after Coomassie-blue staining of the gel. Protein concentration was determined by the method of Bradford (Bradford, 1976).

2.4 Glucose dehydrogenase analysis

2.4.1 Kinetic assays and data processing

Initial velocity studies were performed in 20 mM Tris–HCl buffer pH 8.8, containing 2 M NaCl and 25 mM $MgCl_2$. The reaction was monitored by measuring the appearance of NAD(P)H at 340 nm with a Jasco V-530 spectrophotometer. One unit of enzyme activity was defined as the amount of enzyme required to produce 1 μmol NAD(P)H/min under the assay conditions (40 ºC).

The kinetic constants were obtained from at least triplicate measurements of the initial rates at varying concentrations of D-glucose and $NAD(P)^+$. Kinetic data were fitted to the sequential ordered BiBi equation with the program SigmaPlot 9.0.

2.4.2 Effect of EDTA concentration

The samples at different NaCl concentration were incubated with increasing EDTA concentration for 5 min at room temperature. After the incubation, the residual activities of the enzymes were measured in the activity buffer defined previously (Bonete et al., 1996).

2.4.3 Effect of temperature on enzymatic stability and activity

The samples at different NaCl concentration were incubated at various temperatures: 55, 60, 65, 70 and 80 ºC. Aliquots were withdrawn at given times for measurement of residual activity. Furthermore, enzymatic activity was assayed between 25 and 75 ºC at the same conditions described previously.

2.4.4 Effect of salt concentration on enzymatic activity and stability

The enzymatic activity was measured, as previously described, in buffer with KCl or NaCl in the concentration range of 0-4 M. The results are expressed as the percentage of the activity relative to the highest activity obtained.

Salt concentration stability studies were carried out at room temperature and at 40 ºC. Purified preparations of enzyme in 2 M KCl were quickly diluted with 50 mM potassium phosphate buffer pH 7.3 to obtain 0.25 and 0.5 M KCl concentrations. Samples were removed at known time intervals, cooled on ice, and the residual enzymatic activity was then measured. The results are expressed as the percentage of the activity relative to that existing before incubation.

2.4.5 Differential scanning calorimetry (DSC)

DSC experiments were performed using a VP-DSC microcalorimeter (MicroCal). Temperatures from 40 ºC to 90 ºC were scanned at a rate of 60 ºC/h using 50 mM potassium phosphate buffer pH 7.3 containing 1 mM EDTA and 0.5 M or 2.0 M KCl, which also served

for baseline measurements. Prior to scanning, all samples of protein and buffer were degassed under vacuum using a ThermoVac unit (MicroCal). The protein concentrations were in the range of 50–80 μM (approximately 4–6 mg/ml). The data were analyzed using ORIGIN software v 7.0.

2.5 Isocitrate dehydrogenase analysis

2.5.1 Sequence alignment

Initial alignment with *Hfx. volcanii* NADP-dependent ICDH (Q8X277) was obtained with ClustalW (Thompson et al., 1994), taking account of information of *Bacillus subtilis* (P39126) (Singh et al., 2001) and *E. coli* (P08200) (Hurley et al., 1991) NADP-dependent ICDH, and *Thermus thermophilus* NAD-dependent IMDH (P00351) (Imada et al., 1991) and their sequences. The crystalline structures of all of them were solved previously by high-resolution X-ray analysis. Residues critical to substrate binding were identified from high-resolution crystallographic structures of *E. coli* NADP–ICDH with bound isocitrate (Hurley et al., 1991). Critical residues for coenzyme specificity were identified from high-resolution X-ray crystallographic structures of *E. coli* ICDH complexed with $NADP^+$ (Hurley et al., 1991) and *T. thermophilus* IMDH complexed with NAD^+ (Hurley & Dean, 1994).

Oligonucleotide primers containing the necessary mismatches were used for construction of the mutations: R291S, K343D, Y344I, V350A and Y390P.

2.5.2 Kinetic assays and data processing

The activities of native and mutant ICDHs were determined spectrophotometrically at A_{340} and 30 °C in 20 mM Tris-HCl buffer pH 8.0, 1 mM EDTA, 10 mM $MgCl_2$ (Tris/EDTA/Mg^{2+}) containing 2 M NaCl, 1 mM D,L-isocitrate (Camacho et al., 1995, 2002), with $NADP^+$ or NAD^+ as the coenzyme. One unit of enzyme activity is the reduction of 1 μmol of NADP per min. Initial velocities were determined by monitoring the production of NADPH or NADH at 340 nm in a 1-cm light path, based on a molar extinction coefficient of 6200 M^{-1} cm^{-1}. Kinetic parameters K_m and V_{max} were calculated for the $NADP^+$ and NAD^+ and isocitrate, depending on the cases, and the turnover number (K_{cat}) and catalytic efficiency (K_{cat}/K_m) were determined for each of the mutants, by fitting the data to the Eadie–Hofstee equation with the SigmaPlot program (Version 1.02, Jandel Scientific, Erkath, Germany) (Rodriguez-Arnedo et al., 2005).

2.5.3 Modeling ICDH

Native ICDH and the mutant ICDH with all five amino acids substituted (SDIAP mutant) were modeled with the Swiss-Model program on ExPASy Molecular Biology Server (http://swissmodel.expasy. org/) based on sequence homology. The program uses Blast and ExNRL-3D (derived from PDB) database for the search of a potential protein mold. These proteins, previously resolved by X-ray analysis, with more than 20 amino acids in length and more than 25% sequence identity were chosen. The construction of the structural model was done with the Promodll program and the minimization of energy with Gromos96. The program calculates all levels of identity between the sample problem and the sequence pattern, and it calculates the relative standard deviation to the average of the

corresponding structures models and control. *Hfx. volcanii* ICDH shares 56.6% identity with *E. coli* ICDH (Camacho et al., 2002). The final image was refined with Swiss-Pdb Viewer (Rodriguez-Arnedo et al., 2005).

3. Results

3.1 Analysis of acidic surface of *Hfx. mediterranei* GlcDH

3.1.1 Choice of the halophilic GlcDH mutations

Generally, halophilic enzymes present a characteristic amino acid composition, showing an increase in the content of acidic residues and a decrease in the content of basic residues, particularly lysines. The latter decrease appears to be responsible for a reduction in the proportion of solvent-exposed hydrophobic surface. This role was investigated by site-directed mutagenesis of GlcDH from *Hfx. mediterranei*, in which three surface aspartic residues of the 27 per subunit were changed to lysine residues. At the start of the project, an initial GlcDH structure had been solved at medium resolution. Based on direct observation of this structure, the three aspartic residues chosen were D172, D216 and D344, which at least have the carboxyl oxygens exposed to the solvent (Fig. 1).

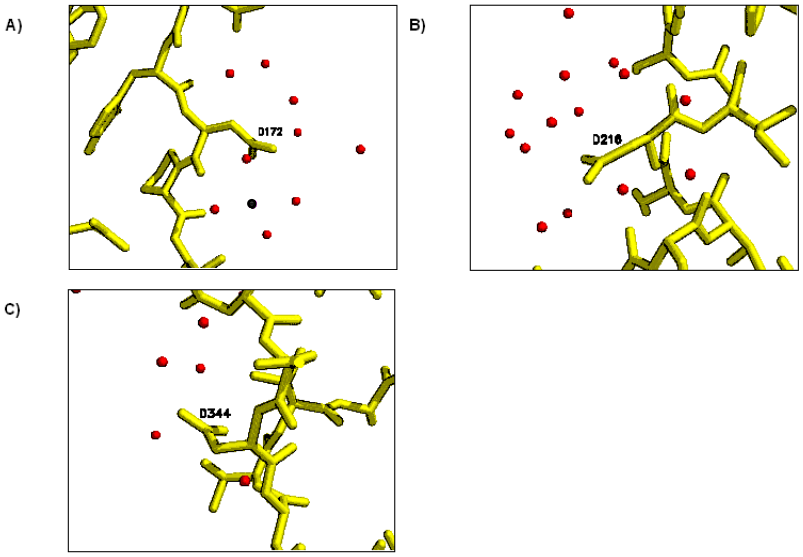

Fig. 1. Diagram showing details of the region surrounding residues D172 (A), D216 (B) and D344 (C) in the high resolution structure of D38C GlcDH with $NADP^+$ and zinc (Britton et al., 2006). The water molecules and the potassium ions are shown in red and black, respectively.

The three selected residues are considered as surface acidic residues, and they are located in different regions of the protein surface. Later, the 1.6 Å resolution GlcDH structure revealed that the side-chain carboxyl of D172 is involved in interactions with a cluster of surface water molecules near a bound potassium counter-ion. In contrast, the side-chain carboxyl of D216 forms interactions with surface waters in a region in which no counter-ions can be

seen. The side-chain carboxyl of D344 lies on the surface, where it interacts with the solvent but also makes hydrogen bonds to the nearby side-chains of T346 and T347. Moreover, multiple alignments (data not shown) with other GlcDH sequences belonging to the MDR superfamily have shown that the acidic residue D216 from *Hfx. mediterranei* GlcDH is conserved in all other halophilic microorganisms. However, residue D344 is only conserved in the *Hfx. volcanii* GlcDH; and residue D172 is not present in any halophilic GlcDH. At the locations corresponding to D172, D216 and D344 in wild type *Hfx. mediterranei* GlcDH, there are non-acidic residues in 100% of the non-halophilic GlcDH sequences analyzed. Therefore, the presence of these acidic residues in the GlcDH from *Hfx. mediterranei* could be an adaptive response to the halophilic environment (Esclapez et al., 2007).

3.1.2 Site-directed mutagenesis and expression of the mutant proteins

Four mutant enzymes were obtained, the triple mutant and the three corresponding single mutant. The triple mutant GlcDH was created with the GeneEditorTM *in vitro* Site-Directed Mutagenesis System (Promega) by introducing the mutations one by one. The single mutant D172K was achieved as the first step in the constructions of the triple mutant GlcDH. The mutants D216K and D344K were constructed by PCR using *Pfu Turbo* DNA polymerase and following digestion with the endonuclease *Dpn*I.

The four mutant genes were cloned into the pET3a expression vector, and the resulting constructs were transformed into *E. coli* BL21(DE3). The expression assays were performed as described previously (Pire et al., 2001). The four mutant proteins were obtained as inclusion bodies, which were solubilized using 20 mM Tris–HCl buffer pH 8.0, 8 M Urea, 50 mM DTT and 2 mM EDTA, like wild type GlcDH. The refolding of each mutant protein was achieved by rapid dilution in 20 mM Tris–HCl buffer pH 7.4, 1 mM EDTA and KCl or NaCl in the concentration range of 1–3 M. The wild-type and triple mutant GlcDHs behave identically in the refolding process under the conditions assayed. The profiles for the triple mutant protein are like the wild type GlcDH, independently of concentration and type of salt. The three single mutants also presented the same profiles. In the presence of NaCl, the recovery of activity was always higher than with KCl; and the highest enzymatic activity was obtained at 3 M NaCl. Furthermore, at low salt concentrations the recovery of activities were lower than at high salt concentrations. No activity was recovered at 1 M KCl or NaCl. Thus, the mutations introduced on the protein surface did not appear to affect refolding in either the triple mutant or the single mutant proteins.

The purification of the GlcDH mutants were carried out as described previously. However, after 3–4 days, protein precipitation was observed in the fractions of triple mutant GlcDH whose protein concentration was greater than 1 mg/ml. This problem was solved by decreasing the protein concentration or by reducing the salt concentration through dialysis against the buffer containing 1 M NaCl or KCl. This fact indicates that the halophilic properties of the triple mutant protein have been altered, since the wild-type and single mutant proteins were stable for months under these conditions.

3.1.3 Properties of the mutant enzymes

The kinetic parameters of the mutant proteins were determined and compared to those that had previously been obtained with wild-type GlcDH. Their K_m values for $NADP^+$ and glucose are essentially similar and no significant differences in the values for V_{max} were

detected. These results indicated that the kinetic parameters were not affected by the mutations. It is unlikely, therefore, that the mutations in position 172, 216 and 344 influenced the active site or the integrity of the enzyme. Similar results were obtained when residues on the surface were mutated on malate dehydrogenase from *Haloarcula marismortui* (Madern et al., 1995) and dihydrolipoamide dehydrogenase from *Hfx. volcanii* (Jolley et al., 1997).

The dependence of enzymatic activity on the concentration of NaCl is shown in Fig. 2. The triple mutant GlcDH shows its maximum activity in a buffer with 0.50–0.75 M NaCl while the wild-type protein has its maximum activity with 1.5 M NaCl. Furthermore, at low salt concentrations the activity of the triple mutant enzyme is higher than the activity of the wild-type GlcDH. At higher salt concentrations, it is lower than the wild-type protein. With the purpose of determining if the observed behavior in the triple mutant protein is due to the presence of just one mutation or of the three modifications, these experiments were also performed with each single mutant protein. The mutants D172K GlcDH and D216K GlcDH show the same profiles as the triple mutant enzyme. In striking contrast, the behavior of the D344K mutant protein is very similar to the profile obtained with the wild-type GlcDH. These results suggest that the D344K modification does not disturb the halophilic characteristics of GlcDH. Therefore, the behavior of the triple mutant GlcDH in the salt concentrations assayed could be due to the introduction of the mutation D172K and D216K. The profiles obtained using buffers with KCl are very similar.

At optimal salt concentration, the activities of the wild-type and mutant GlcDH proteins are very close. The kinetic parameters are very similar too. Therefore, it appears that the different mutations introduced in GlcDH only influence the dependence of enzymatic activity on the salt concentration. However, in similar studies with the dihydrolipoamide dehydrogenase from *Hfx. volcanii*, mutants with only one mutation (E243Q, E423S or E423A) resulted in enzymes less active than the wild-type enzyme and with different kinetic parameters. Based on these results, Jolley and co-workers (Jolley et al., 1997) also supported the view that it is the precise structural organization of acidic residues that is important in halophilic adaptation and not only the increase in acidic residue content (Madern et al., 1995; Irimia et al., 2003).

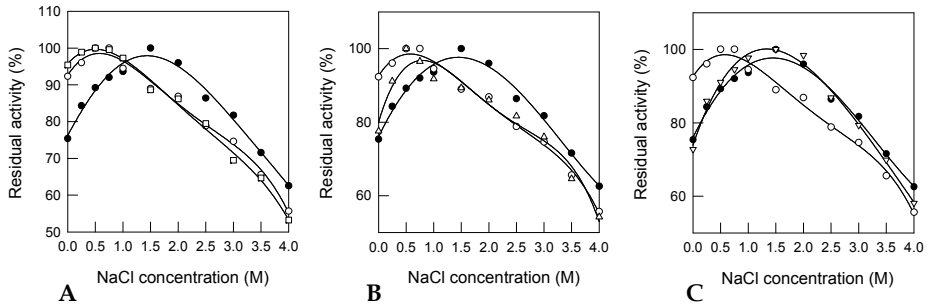

Fig. 2. Effect of NaCl on the activity of wild-type GlcDH (•), triple mutant GlcDH (○) and single mutants: (A) D172K GlcDH (□), (B) D216K GlcDH (△) and (C) D344 K GlcDH (▽). The activity buffer was 20 mM Tris–HCl pH 8.8 with varying concentrations of NaCl.

The effects of different salt concentrations on the residual activity of wild-type halophilic GlcDH and the four mutant proteins were measured after incubation at 25 ºC and 40 ºC. In the presence of 2 M KCl, neither wild-type enzyme nor mutant proteins were inactivated at the temperatures assayed. In particular, at salt concentrations above 1 M, the proteins were stable for weeks. As salt concentration increases, the proteins were more stable independent of the temperature. However, at low salt concentrations, small differences were observed in the stability of the proteins. The triple mutant and each single mutant protein appeared to be slightly more stable than the wild-type protein at 0.25 and 0.50 M KCl. The behavior of the proteins at 25 ºC was similar, although a decrease in the temperature implies an increase of the period over which the enzymes are stable. The half-life time ($t_{1/2}$) for each protein was calculated (Table 1) showing that the mutant protein half-life times, either as a single alteration or altogether, are longer than wild type, both at 25 ºC and 40 ºC. However, there are no significant differences between the triple mutant and the single mutant proteins. All showed similar half-life times under the conditions assayed.

Biocalorimetry experiments were carried out under two different KCl concentrations using a DSC. In the presence of 2 M KCl, wild-type and single mutant GlcDH denaturing temperatures range from 74.6 ºC to 75.9 ºC. However, the triple mutant enzyme shows a lower denaturing temperature, between 73.6 ºC and 73.7 ºC. In other words, the triple mutant enzyme is denatured at slightly lower temperatures than are the wild-type and single mutant GlcDHs in the presence of high salt. At 0.50 M KCl (low salt), the results obtained do not reveal significant data; but the protein denaturing temperatures are lower than those obtained in the presence of high salt, independent of protein type (Fig. 3). This decrease was expected because the halophilic proteins are destabilized in low salt. Consequently the denaturing temperatures of the wild-type and mutant enzymes ranged from 59.8 ºC to 60.7 ºC. There were no significant differences between the temperatures.

	"Wild type"	**Triple mutant**	**D172K**	**D216K**	**D344K**
$t_{1/2}$ **40 ºC (h)**					
0.25 M KCl	14 ± 2	18 ± 3	23 ± 5	26 ± 8	25 ± 4
0.50 M KCl	86 ± 4	114 ± 9	95 ± 9	117 ± 8	114 ± 7
>1.0 M KCl	>170	>170	>170	>170	>170
$t_{1/2}$ **25 ºC (h)**					
0.25 M KCl	142 ± 22	246 ± 23	293 ± 30	219 ± 32	232 ± 30
0.50 M KCl	506 ± 50	613 ± 74	630 ± 113	660 ± 113	537 ± 75
>1.0 M KCl	>170	>170	>170	>170	>170

Table 1. Half-life times of "wild type" and mutant GlcDHs in the presence of different KCl concentrations at 40 ºC (A) and 25 ºC (B).

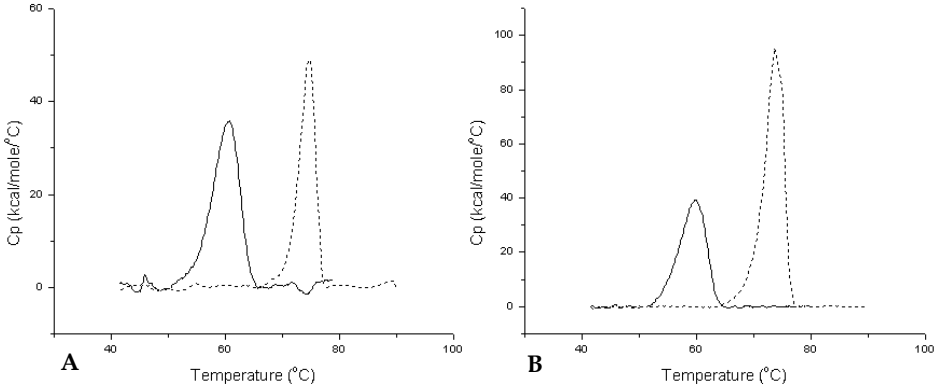

Fig. 3. Calorimetric traces of the thermal transition for wild-type GlcDH (A) and triple mutant GlcDH (B). Thermal transitions were determined in 50 mM potassium phosphate buffer pH 7.3 with 0.5 M (continuous line) or 2 M KCl (dotted line).

The data that we have presented indicate that the halophilic properties of the mutant proteins have been modified. Their enzymatic activity and kinetic parameters have been not affected by the mutations. The triple mutant and the single mutants, D172K GlcDH and D216K GlcDH, have reached their maximum activities at lower salt concentrations than wild-type GlcDH and the D344K mutant. It appears that the D344K substitution has no effect on the salt activity profile. Strikingly, in all the cases the mutant proteins were slightly more stable at low salt concentrations than was the wild-type GlcDH , although they require high salt concentration for maximum stability, like a malate dehydrogenase mutant from *Har. marismortui* (Madern et al., 1995). The biocalorimetry analyses have revealed another difference. The single mutant and the wild-type GlcDHs showed similar denaturing temperatures in the presence of 2 M KCl, while the triple mutant enzyme presented a lower denaturing temperature. Thus, more than one of our substitutions are apparently needed to significantly modify the protein's denaturing temperature at high salt concentration. Probably, these data are the result of an alteration of the hydration shell, which is required for halophilic proteins to be stable at high salt concentrations. Analysis of the high resolution GlcDH structure has shown that the size and order of the hydration shell in the halophilic enzyme is significantly greater than in non-halophilic proteins. Analyses also show that the differences in the characteristics of the molecular surface arise not only from an increase in negative surface charge, but also from the reduction in the percentage of hydrophobic surface area due to lysine side chains. Lysine residues of halophilic enzymes tend to be more buried than those of non-halophilic proteins (Britton et al., 2006).

3.2 Analysis of the zinc-binding site of GlcDH from *Hfx. mediterranei*

3.2.1 Choice of the GlcDH mutations

Whilst sequence analysis clearly identifies *Hfx. mediterranei* GlcDH as belonging to the zinc-dependent medium chain dehydrogenase/reductase family, the zinc-binding properties of the enzymes of this family are known to vary. The family includes numerous

zinc-containing dehydrogenases, which bind one or two zinc atoms per subunit. One of the zinc atoms is essential for catalytic activity, while the other has a structural role and is not present in all the family members. Previous biochemical studies established that the *Hfx. mediterranei* GlcDH appears to have a single zinc atom per subunit. The role of this zinc atom is to participate in the catalytic function of the enzyme (Pire et al., 2000; Pire et al., 2001).

In the crystal structure of horse liver alcohol dehydrogenase (HLADH), three protein ligands, C46, H67 and C174 coordinate the catalytic zinc (Eklund et al., 1981). Residues analogous to C46 and H67 are conserved in the vast majority of members of the MDR family, while in some enzymes the analogous residue for C174 is glutamate as in *Thermoplasma acidophilum* GlcDH (Fig. 4). On the basis of sequence alignment, the residues involved in binding the catalytic zinc in *Hfx. mediterranei* GlcDH are predicted to be D38, H63 and E150. This sequence pattern of residues that bind the catalytic zinc has not previously been observed for any enzyme in the MDR family. The change of the C38 to D38 in the halophilic enzyme could be an adaptive response to the halophilic environment.

In order to investigate the mode of zinc binding to the halophilic GlcDH, two mutant enzymes were constructed by site-directed mutagenesis. We replaced the D38 present in the active center of the protein with C or A.

3.2.2 Site-directed mutagenesis and expression of the mutant proteins

Site-directed mutagenesis was carried out to replace the D38 residue by cysteine and alanine in the recombinant GlcDH using GeneEditorTM *in vitro* Site-Directed Mutagenesis System. The mutant genes were cloned into the pET3a expression vector. The resulting constructs were introduced by transformation into *E. coli* BL21(DE3). After expression, both mutant proteins were obtained as inclusion bodies, as was wild-type GlcDH.

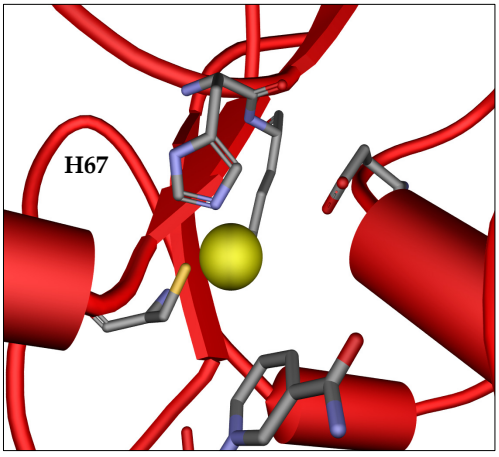

Fig. 4. The catalytic zinc-binding site in *Thermoplasma acidophilum* GlcDH.

The mutant enzymes were refolded and purified as described previously (Pire et al., 2001). In both mutants, the activity was lower than that of the wild-type protein, with the D38A mutant being inactive. This result suggests that D38 is an important residue and that the mutation to A38 leaves the enzyme seriously compromised. With respect to the D38C mutant, the maximum activity observed was approximately 30% of the activity of the wild-type enzyme.

3.2.3 Characterization of D38C GlcDH

The kinetic parameter values for mutant D38C GlcDH were determined and compared with those obtained for wild-type GlcDH (Table 2). K_{mNADP^+} differences are not significant; however, the mutation led to a significant increase of the K_m for glucose. Moreover, as the K_{cat} and $K_{cat}/K_{mglucose}$ parameters show, the catalytic efficiency of the mutant protein is less than the catalytic efficiency of wild-type GlcDH. These results indicate that the replacement of D38 to C38 in the GlcDH probably affects not only the catalytic zinc-binding site, but also the active site of the protein. The C38 GlcDH decreases the enzyme's affinity for glucose and its V_{max} relative to the wild-type enzyme. Consequently, the catalytic efficiency of the mutant enzyme is reduced.

	K_{mNADP^+} (mM)	$K_{mglucose}$ (mM)	V_{max} (U/mg)	K_{cat} (min^{-1})	K_{cat}/K_m ($mM^{-1}min^{-1}$)
"Wild type"	0.035 ± 0.004	2.8 ± 0.3	397 ± 15	31 ± 1	11.10 ± 1.6
D38C	0.044 ± 0.010	12.4 ± 2.3	83 ± 9	7 ± 1	0.52 ± 0.14

Table 2. Kinetic parameters of recombinant wild-type GlcDH and the D38C mutant.

The zinc ion in the wild-type enzyme can be removed by EDTA treatment to yield an inactive enzyme (Pire et al., 2000). In order to compare the strength of zinc binding in "wild type" and in the D38C mutant, a similar treatment was carried out. Fig. 5 shows that zinc is more weakly bound in the D38C mutant than in the wild-type enzyme. The EDTA concentration needed to inactivate the enzyme is lower than that needed for the wild-type enzyme, and this inactivation was independent of salt concentration. For the wild-type enzyme, the capacity of EDTA to sequester the zinc is lower in the D38C mutant; and it is salt concentration-dependent. In the three NaCl concentration tested, the enzyme lost approximately 80% of its activity in the presence of 0.25 mM EDTA, and it was completely inactive at concentrations higher than 2 mM. However, in the case of the wild-type GlcDH, the EDTA necessary to sequester zinc atom at 3 M NaCl is higher than at 1 M, so the behavior of this protein is dependent on the salt concentration. At concentrations above 4 mM of the chelating agent, the enzyme is completely inactive, regardless of the NaCl concentration. Therefore, the substitution of D38 by C38 in the protein has weakened the binding of zinc ion. The D residue at position 38 in the halophilic glucose dehydrogenase instead of C, which is commonly found at the analagous postion in other members of the medium chain dehydrogenase family, could represent a halophilic adaptation.

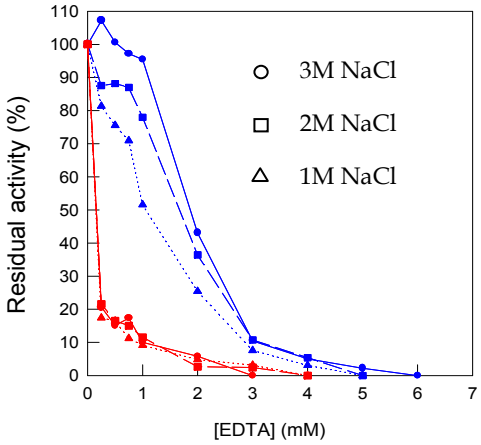

Fig. 5. Deactivation of the wild-type (blue) and D38C mutant (red) GlcDH under various EDTA concentrations at different buffer salt concentrations.

The replacement of D38 by C38 makes the binding of catalytic zinc ion of the halophilic GlcDH very similar to that presented by the thermophilic GlcDHs and other MDR family proteins. In order to clarify if C38 instead of D38 modifies the thermal characteristics of the enzyme at different salt concentrations, the effect of the temperature on enzymatic stability and activity were determined.

Generally at low salt concentration, halophilic proteins are less stable. High temperatures can contribute to their destabilization under these conditions. At high salt concentrations, halophilic proteins are stable; but stability can be perturbed by several factors, such as high temperatures. The thermal inactivation results illustrate that both the wild-type and the D38C mutant proteins show higher thermostability when the concentration of NaCl is raised. However, the D38C GlcDH appears to be slightly more thermostable than "wild type" GlcDH at the NaCl concentration assayed. The half-lives calculated for each protein under the different conditions are shown at Table 3. In general, at temperatures of 60-70 ºC the D38C mutant shows a half-life higher than that of wild-type GlcDH. No reliable comparisons can be made at 80 ºC, as at that temperature total inactivation of the enzyme is achieved in a few seconds. Below 60 ºC the differences between the half-lives are not significant.

	$t_{½}$ 1 M NaCl (h)		$t_{1/2}$ 2 M NaCl (h)		$t_{1/2}$ 3 M NaCl (h)	
	D38C	**"Wild type"**	**D38C**	**"Wild type"**	**D38C**	**"Wild type"**
55 ºC	33.9	37.2	(a)	(a)	(a)	(a)
60 ºC	7.4	4.6	123.7	51.33	210.6	96.27
65 ºC	0.3	0.3	9.6	8.3	(a)	(a)
70 ºC	(b)	(b)	0.3	0.2	17.2	8.25
80 ºC	(b)	(b)	0.04	0.02	0.2	0.2

(a) The enzyme is stable under these conditions.
(b) The enzyme is stable for only a few minutes under these conditions.

Table 3. Half-life time at different temperatures and salt concentrations of wild-type GlcDH and D38C GlcDH.

The replacement of D38 by C38 appears to have a stabilizing effect on the ability of the protein to withstand high temperatures, producing an enzyme that is marginally more stable at high temperature. However, it is clear that the enzymatic activity of the mutant is lower.

3.3 Alteration of coenzyme specificity in *Hfx. mediterranei* GlcDH and *Hfx. volcanii* ICDH

3.3.1 *Hfx. mediterranei* GlcDH

3.3.1.1 Mutations for the reversal of coenzyme specificity

The ability of dehydrogenases to discriminate between NAD^+ and $NADP^+$ lies in the amino acid sequence of the nucleotide-binding βαβ motif. This βαβ motif is centered around a highly conserved Gly–X–Gly–X–X–Gly sequence (where X is any amino acid) connecting the first β strand to the α helix. The presence of an aspartic residue at the C-terminal end of the second β strand is conserved in NAD^+-specific enzymes. In many $NADP^+$-specific enzymes, this residue is replaced by a smaller and neutral residue and complemented by a nearby positively charged residue that forms a positively charged binding pocket for adenosine 2′-phosphate. The three-dimensional structure of the cofactor binding-site of *Hfx. mediterranei* GlcDH (Fig. 6) indicates the spatial location of the residues mutated here and the interaction of R207 and R208 with the 2′-phosphate group of $NADP^+$ (Britton et al., 2006; Pire et al., 2009).

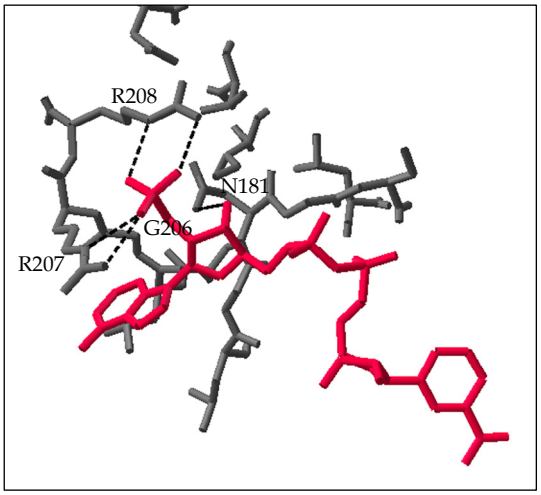

Fig. 6. View of $NADP^+$ bound to "wild type" GlcDH. Interaction through hydrogen bonds is represented with dotted lines. $NADP^+$ is shown in red; a portion of GlcDH, in gray. Crystal structure of GlcDH is from *Hfx. mediterranei* (PDB code 2B5V, Britton et al., 2006).

3.3.1.2 Protein properties

All the reversal coenzyme specificity mutants were expressed as inclusion bodies, and refolding was carried out by rapid dilution in the same way as for the wild-type enzyme

(Pire et al., 2001). To assess that the enzymes reached their maximum activity in terms of proper refolding, enzyme activity was measured as a function of time after rapid dilution. The wild-type and mutated enzymes behaved similarly during refolding, although the refolding kinetics of the mutants were slower. Maximum activity was reached after approximately 24 h with the mutated enzymes, whereas the wild-type enzyme achieved maximum activity 2 h after the rapid dilution of solubilized inclusion bodies (Pire et al, 2009).

Once the protein was folded, the purification procedures were identical for the wild-type and mutant enzymes (Pire et al., 2001).

3.3.1.3 Kinetics of "wild type" and coenzyme specificity reversal mutant enzymes

The kinetic constants of the wild-type and mutant forms of GlcDH were determined with both coenzymes, NAD^+ and $NADP^+$. The kinetic constants for the enzymes are compared in Table 4 A and B.

The K_m value of the wild-type enzyme was 11-fold lower for $NADP^+$ than for NAD^+, indicating that the enzyme has a strong preference for $NADP^+$. The single substitution G206D increased the K_m 74-fold for $NADP^+$ and decreased K_{cat} 2-fold, resulting in a 150-fold decrease in the K_{cat}/K_m when using $NADP^+$. This was to be expected as the negative charge of D206 would be likely to repel the adenosine 2′-phosphate of $NADP^+$. This single substitution had a positive effect on catalysis with NAD^+. In NAD^+-dependent enzymes, an aspartic residue in this position confers specificity towards NAD^+ by the bidentate hydrogen bonding with the 2′ and 3′ hydroxyl groups of the adenosine of NAD^+. The K_m in the presence of NAD^+ was similar to that of the "wild type", but K_{cat} showed a 2-fold increase. The G206D mutant preferred NAD^+ to $NADP^+$, showing a K_{cat} value with NAD^+ similar to that of the wild-type enzyme with $NADP^+$; however, the K_{cat}/K_m ratio was still better in the wild-type enzyme with $NADP^+$.

The single mutant R207I showed an increase of 48 times in K_m value with $NADP^+$ when compared with the "wild type"; this again was as expected, considering the role of D207 in the stabilization of the negative charge of the adenosine 2′-phosphate group of $NADP^+$. This increase was accompanied by a decrease in K_{cat}, which clearly makes the R207I mutant less efficient in catalysis with $NADP^+$. For NAD^+ the K_m value also increased, but at a ratio of 3 times, much lower than the K_m increase with $NADP^+$. The R207I substitution also makes the enzyme less efficient with NAD^+, with a decrease of 4 times in K_{cat}/K_m; this substitution also increases the K_m for glucose. A similar effect was even more pronounced in the single substitution R208N, in which saturation with glucose cannot be achieved, and attempts to calculate K_m and K_{cat} with both coenzymes led to very high standard deviation values.

The activity of the G206D/R207I double mutant with $NADP^+$ was very low (almost undetectable), and as such the kinetic parameters could not be calculated. However, when the coenzyme NAD^+ was incubated with this double mutant, it reached the highest K_{cat} value, between 1.5 and 2 times higher than the K_{cat} of the wild-type enzyme with $NADP^+$, and between 3 and 4 times higher than the K_{cat} of the "wild type" with NAD^+. These values indicate that the local rearrangement of the active centre due to the mutations makes catalysis more efficient. The dissociation constant for NAD^+ in the double mutant decreased 1.7-fold in comparison with K_{iNAD+} in the "wild type", but the K_{mNAD+} value of NAD^+ registered a 2-fold increase. The G206D/R207I/R208N triple substitution produced an

A)	$NADP^+$ Wild type	G206D	R207I
$K_{iNAD(P)^+}$ (mM)	0.09 ± 0.02	0.69 ± 0.10	1.3 ± 0.5
$K_{mNAD(P)^+}$ (mM)	0.035 ± 0.009	2.6 ± 0.4	1.7 ± 0.3
$K_{mglucose}$ (mM)	2.8 ± 0.3	52 ± 8	24 ± 8
$^aK_{cat}$ (min^{-1}) ($x10^{-3}$)	31.1 ± 1.2	15.7 ± 1.5	11.8 ± 1.5
$K_{cat}/K_{mNAD(P)^+}$ ($mM^{-1}min^{-1}$) ($x10^{-3}$)	900 ± 30	6.0 ± 1.5	7 ± 2
$K_{cat}/K_{mglucose}$ ($mM^{-1}min^{-1}$) ($x10^{-3}$)	11.1 ± 1.6	0.30 ± 0.07	0.5 ± 0.2

B)	NAD^+ Wild type	G206D	R207I	G206D/ R207I	G206D/R207I/ R208N
$K_{iNAD(P)^+}$ (mM)	2.0 ± 0.2	1.0 ± 0.2	2.1 ± 0.9	1.17 ± 0.13	1.7 ± 0.4
$K_{mNAD(P)^+}$ (mM)	0.40 ± 0.12	0.49 ± 0.16	1.3 ± 0.4	2.7 ± 0.6	1.3 ± 0.3
$K_{mglucose}$ (mM)	12.9 ± 1.4	15 ± 4	32 ± 13	80 ± 14	57 ± 11
$^aK_{cat}$ (min^{-1}) ($x10^{-3}$)	15.8 ± 0.9	34 ± 5	4.3 ± 0.8	54 ± 7	2.8 ± 0.3
$K_{cat}/K_{mNAD(P)^+}$ ($mM^{-1}min^{-1}$) ($x10^{-3}$)	44 ± 17	70 ± 30	3.3 ± 0,6	20 ± 7	2.1 ± 0.7
$K_{cat}/K_{mglucose}$ ($mM^{-1}min^{-1}$) ($x10^{-3}$)	1.2 ± 0.2	2.3 ± 0.9	0.13 ± 0.08	0.7 ± 0.2	0.049 ± 0.015

Substrate concentrations range used in kinetic parameters determination: Wild-type: [glucose]= 2-20 mM, [$NADP^+$]= 0.04-0.2 mM, [NAD^+]= 0.286-1mM; G206D: [NAD^+]= 0.286 -1mM, [glucose]= 2.5-20 mM, [$NADP^+$]= 0.286-4 mM, [glucose]= 2.5-40 mM; R207I: [NAD^+]= 0.8-2 mM, [glucose]= 25-100 mM, [$NADP^+$]= 0.4-2 mM, [glucose]= 20-100 mM; G206D/R207I: [NAD^+]= 0.4-4 mM, [glucose]= 10-100 mM; G206D/R207I/R208N:[NAD^+]= 0.8-4 mM, [glucose]= 16.67-100 mM.
$^aK_{cat}$ values are referred to the GlcDH dimer kinetic parameters and are expressed ± standard deviation.

Table 4. Kinetic constants of wild-type and mutant GlcDH.

inactive enzyme with $NADP^+$, confirming that these two arginines are necessary for $NADP^+$ stabilization. Regarding the kinetic parameters with NAD^+, as in the double mutant G206D/R207I, the K_m values of both substrates were higher than in the "wild type"; but in the triple mutant the K_{cat} was also lower, and it was the worst catalyst.

In contrast with our results, in alcohol dehydrogenase from gastric tissues of *Rana perezi*, the complete reversal of coenzyme specificity from NADP(H) to NAD(H) was reached with the concerted mutation of three residues G223D/T224I/H225N (Rosell et al., 2003) . The single mutation G223D had no effect on catalysis with NAD^+ and the double mutant G223D/T224I was a better catalyst than the single mutant with NAD^+, but worse than the triple mutant. The great increase in the K_{cat} observed with the GlcDH double mutant was not observed in alcohol dehydrogenase. It appears that one or two substitutions in alcohol dehydrogenase were not sufficient to transform coenzyme specificity, whereas multiple substitutions could be effective (Rosell et al., 2003). The same, but reverse, effect was observed with NAD^+-dependent xylitol dehydrogenase, in that the reverse of coenzyme specificity from NAD^+ to $NADP^+$ was achieved with the triple mutant D207A/I208R/F209S (Watanabe et al., 2005). In yeast alcohol dehydrogenase, a NAD^+ specific enzyme, the D201G substitution produces an

enzyme with low activity with $NADP^+$, but the G203R substitution neither affects affinity for NAD^+ or NADH nor enables reactivity with $NADP^+$, and the D201G/G203R enzyme has kinetic characteristics similar to the single D201G enzyme. R203 should be able to interact with the 2'-phosphate, but it seems that a greater change is required in the amino acid sequence to transform the specificity (Fan & Plapp, 1999).

Although there are some examples of a coenzyme specificity change from NAD^+ to $NADP^+$ with only one mutation, it seems that the specificity change from $NADP^+$ to NAD^+ is more difficult to reach with single substitutions. This study shows that G206, R207 and R208 are determinant for coenzyme specificity in *Hfx. mediterranei* GlcDH. The substitution G206D hampered the binding of $NADP^+$ and increased by a factor of two the activity with NAD^+, resulting in an enzyme that preferred NAD^+ over $NADP^+$. Double mutation G206D/R207I was enough to make an unproductive enzyme with $NADP^+$, although the more important findings were that in double mutant G206D/R207I, the specific activity of the enzyme with NAD^+ was almost twice than in the wild type with $NADP^+$, though the K_{cat}/K_m ratio was low due to the increase of K_m. In this sense, as some authors point out, we have to be cautious to interpret the K_{cat}/K_m ratio as catalytic efficiency, since at certain substrate concentrations the wild-type GlcDH catalyzes the oxidation of glucose, using $NADP^+$ as a coenzyme at a lower rate than double mutant in the presence of NAD^+ (Pire et al., 2009)

3.3.2 *Hfx. volcanii* ICDH

One of the most interesting features of proteins is the fact that they keep in their amino acid sequences a substantial record of their evolutionary histories. Surprisingly, homologous proteins in organisms that diverged billions of years are still similar enough to recognize a correspondence in the organization of conserved and variable regions. They can even be used as markers of the evolutionary process itself. Such comparisons have been performed using protein sequence alignments obtained with different algorithms. The alignments may reveal amino acids with a common origin and/or having similar positions in the corresponding three-dimensional structures of each protein.

Molecular evolution is based on the use of alignments to reconstruct gene trees representing, as closely as possible, the historic process of sequence divergence. This reconstruction requires the development of statistical models able to reproduce the process of mutation, drift and selection.

If one represents the structural alignment of a family of proteins in the form of linear sequence of amino acids, one can see that the spatial correspondence of identical amino acids is reflected in the form of sequence identity. The presence of insertions and deletions of specific parts of structure is revealed in the form of holes or gaps (Gómez-Moreno & Sancho, 2003).

The aim of alignment algorithms for amino acid sequences is the relative structural correspondence of residues. Comparative modeling is the extrapolation of the structure to a new amino acid sequence (model) from a known three-dimensional structure of at least one member (mould) of the same family of proteins. The obtained models contain sufficient information to permit experimental design with an acceptable degree of reliability or to allow structural comparison (Gómez-Moreno & Sancho, 2003).

One of the purposes of such an analysis is to select residues for mutation that may cause changes in some of the biochemical characteristics of the protein, such as the variation in coenzyme specificity.

3.3.2.1 Sequence alignment

The ICDHs belong to an ancient and divergent family of decarboxylating dehydrogenases that includes NAD-isopropylmalate dehydrogenase (IMDH) (Dean & Golding, 1997). "This family of dehydrogenases shares a common protein fold, topologically distinct from other dehydrogenases of known structure that lacks the αβαβ binding motif characteristic of the nucleotide-binding Rossman fold (Rossman et al., 1974; Chen et al, 1995). In ICDHs the adenosine moiety of the coenzyme binds in a pocket constructed from two loops and an α-helix (Hurley et al., 1991), although the latter is substituted by a β-turn in IMDH (Imada et al., 1991; Chen et al., 1995).

Dehydrogenases discriminate between nicotinamide coenzymes through interactions established between the protein and the 2′-phosphate of $NADP^+$ and the 2′- and 3′-hydroxyls of NAD^+ (Chen et al., 1995). In the NAD-binding site, the introduction of positively charged residues changes the preference of an NAD-dependent enzyme to neutralize the negatively charged 2′-phosphate of $NADP^+$, as it has been demonstrated with engineered dihydrolipomide and malate dehydrogenases (Bocanegra et al., 1993; Nishiyama et al., 1993).

Specificity in *E. coli* ICDH is conferred by interactions among R395, K344, Y345, Y391 and R292′ with the 2′-phosphate of bound $NADP^+$ (Hurley et al., 1991; Dean & Golding, 1997). These residues are conserved in oligomeric NADP-dependent ICDHs and some monomeric NADP–ICDHs from prokaryotes. They are replaced with a variety of residues in the NAD-dependent ICDHs (Lloyd & Weitzman, 1988; Steen et al., 1997; Yasutake et al., 2003). Except for the substitution of Y391 with glutamine in *Aeropyrum pernix*, these residues are conserved in the archaeal NADP-dependent ICDHs and are in accordance with the cofactor specificity (Steen et al., 2002). However, K344 and Y345, which interact with $NADP^+$ in ICDH, are substituted by D278 and I279 in IMDH. This enzyme preferentially uses NAD^+ as a coenzyme; and D278 hydrogen bonds to the 2′-hydroxyl group of NAD^+, while repelling the 2′-phosphate of $NADP^+$ (Chen et al., 1996; Hurley et al., 1996). Thus, this residue is a major determinant of coenzyme specificity toward NAD+ and is strictly conserved in all known IMDHs (Chen et al., 1996). The specificity in IMDH is conferred by the strictly conserved D278 (D344 in ICDH numbering), which forms a double hydrogen bond with the 2′- and 3′-hydroxyls of the adenosine ribose of NAD^+ (Dean & Golding, 1997). Not only are these movements incompatible with the strong 2′-phosphate interactions seen in NADP-ICDH, but the negative charge on D344 may also repel $NADP^+$ (Hurley et al., 1996; Rodriguez-Arnedo et al., 2005).

Specificity is governed by (1) residues that interact directly with the unique 2′-hydroxyl and phosphate groups of NAD^+ and $NADP^+$, respectively; (2) more distant residues that modulate the effects of the first group; and (3) remote residues (Hurley et al., 1996). The first group of residues includes L344, Y345, Y391 and R395 (*E. coli* ICDH numbering), and it is easy to imagine that changes at these residues destroy the 2′-phosphate binding site (Hurley et al., 1996). The second group of residues includes V351. The adenine ring of NAD^+ approaches the C_α of residue 351 as a result of a conformational change in the adenosine

ribose of NAD^+, which also brings it close to D344, suggesting an important role for the ring shift in specificity. The V351A mutant was designed to avoid obstructing this ring shift. A second key role for V351A is to accommodate the correct packing of the introduced I345 (Hurley et al., 1996). Sequence alignment of *Hfx. volcanii*, *E. coli* and *B. subtilis* NADP-dependent ICDHs with *T. thermophilus* NAD-dependent IMDH (Fig. 7) showed that amino acid residues involved in $NADP^+$ binding are conserved in the NADP-dependent ICDHs and are located in a characteristic binding pocket constructed from two loops and an α-helix. In IMDH from *T. thermophilus*, this pocket comprises two loops and a β-turn (Dean & Golding, 1997; Rodriguez-Arnedo et al., 2005).

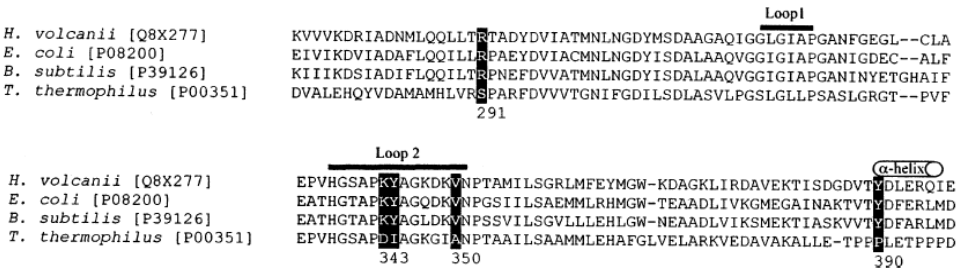

Fig. 7. Sequence alignments of *Hfx. volcanii*, *E. coli* and *B. subtilis* NADP-dependent isocitrate dehydrogenases (ICDHs) and *T. thermophilus* NAD-dependent isopropylmalate dehydrogenase. Amino acids critical to coenzyme binding and catalysis are enclosed in black boxes, and numbers correspond to relative position in the ICDH sequence from *Hfx. volcanii.*

3.3.2.2 Site-directed mutagenesis

In the halophilic enzyme, the R291S, K343D, Y344I, V350A and Y390P (halophilic ICDH numbering) mutations were selected based on homology. The substitutions were made by site-directed mutagenesis. The changes carried out are positively charged residues, such as Arg and Lys; uncharged amino acids, such as Ser; or negatively charged, such as Asp. Lys is a residue that appears to be conserved in many species, which could mean that its positive charge is crucial for proper catalysis by the enzyme. The first mutant made and characterized was R291S. Arg forms a hydrogen bond with the 2′-phosphate of a $NADP^+$, as can be seen in the *E. coli* ICDH structure, and is replaced by Ser in *T. thermophilus* IMDH and by a wide variety of amino acids in other NAD-dependent enzymes (Chen et al., 1995). We found that, after the R291S substitution in *Hfx. volcanii* ICDH, the specificity for $NADP^+$ decreased; but no activity for NAD^+ was detected. The double mutant was obtained with a second mutation at residue Y390 in the halophilic enzyme (Rodriguez-Arnedo et al., 2005). This amino acid was replaced with Pro, as in IMDH from *T. thermophilus* (Chen et al., 1995), in order to remove a hydrogen bond to the 2′-phosphate and alter the local secondary structure from an α-helix to a β-turn. When examined, however, the secondary structure was unchanged by this substitution. Furthermore, preliminary studies (Chen et al., 1995) have shown that it is unnecessary to replace an α-helix by a β-turn to eliminate interactions with the 2′-phosphate of $NADP^+$. Mutants three (SDP mutant) and four (SDIP mutant) involved replacing K343 and Y344 with Asp and Ile, respectively, to obtain triple and quadruple mutants. Both D343 (D278 in IMDH numbering) and I344 (I279 in IMDH

numbering) are found in all known prokaryotic NAD-dependent decarboxylating dehydrogenases (Chen et al., 1996). In *Pyrococcus furiosus* NAD-dependent ICDH, the introduction of the double mutation of D328L/I329Y did not greatly decrease the preference for NAD^+; but it improved the preference for $NADP^+$ by reducing the catalytic efficiency for NAD^+ (Steen et al., 2002). In comparison, the loss of hydrogen bonding and the introduction of a negatively charged Asp greatly reduced binding with $NADP^+$, but the changes had no effect on binding with NAD^+ in *Hfx. volcanii* ICDH. The final mutation was V350A to obtain a quintuple mutant (SDIAP mutant) (Rodriguez-Arnedo et al., 2005).

After all five amino acids were changed in *Hfx. volcanii* ICDH, coenzyme binding switched from $NADP^+$ to NAD^+. The importance of V350A could explain why the quadruple mutation (SDIP mutant) destroyed $NADP^+$ binding without promoting NAD^+ binding. The corresponding residue is Val or Ile in all known NADP-dependent ICDHs and Ala in most, but not all, NAD-dependent dihydrodiol dehydrogenases (Hurley et al., 1996). Coenzyme specificity was changed to NAD^+ only after the fifth mutation, V350A. When V350A was the only change (single mutant), the coenzyme specificity was not switched to NAD^+, although specificity for $NADP^+$ decreased, as occurred when R291S was the only change (Rodriguez-Arnedo et al., 2005).

Molecular models of both the native enzyme and the mutants showed no significant changes in secondary structure when they were compared with the model of *E. coli* ICDH, and with each other (data not shown). The high sequence identity (56.6%) of halophilic organism isocitrate dehydrogenase with that of *E. coli* allows a reasonable model which would present a deviation of 1 Å.

The introduced mutations in ICDH from *Hfx. volcanii* do not produce apparent changes in the structure of the enzyme. Therefore, the change of coenzyme specificity would have occurred by the elimination of the hydrogen bonds formed by the amino acids involved in the binding of $NADP^+$. The position of the $NADP^+$ in the mutant is the same as it is in the native enzyme. The loop formed to accommodate the coenzyme is the same as the one seen in the *E. coli* enzyme. This loop has also been observed in the three-dimensional structure of ICDH from *B. subtilis* (Singh et al., 2001).

3.3.2.3 Kinetic characterization of mutants

Five amino acid substitutions introduced into wild-type *Hfx. volcanii* ICDH caused a complete shift in preference from $NADP^+$ to NAD^+. All mutations were based on sequence homology with NAD-dependent enzymes. Wild-type ICDH showed total dependence on $NADP^+$ and had a Michaelis constant (K_m) of 101 ± 30 μM and a K_{cat} of 0.176 ± 0.020 min^{-1} (Table 5). The affinity for the coenzyme was not changed until all five mutations were made, but specificity for $NADP^+$ decreased after the first mutation. Our SDIAP mutant displayed a preference for NAD^+ over $NADP^+$, had a K_m for NAD^+ of 144 ± 60 μM, and a K_{cat} of 0.0422 ± 0.0017 min^{-1} (Table 5). The K_m for $NADP^+$ increased approximately threefold in the single mutant and remained constant in the three subsequent mutants. The K_{cat}/K_m for the $NADP^+$ coenzyme was reduced 24-fold in the quadruple mutant. In contrast to the results obtained with other NAD(P)-dependent dehydrogenases (Nishiyama et al., 1993; Chen et al., 1997; Steen et al., 2002), our experiments showed that none of the mutants of *Hfx. volcanii* ICDH displayed dual cofactor specificity. Table 5 indicates that the K_{cat} for NAD^+ is lower than the K_{cat} for $NADP^+$ for the wild-type and some mutants, suggesting that most of the changes in

specificity arise from discrimination in binding, rather than direct changes in catalysis. Catalytic efficiency of the quintuple mutant (SDIAP) with NAD^+ was 17% of that of the wild-type enzyme with $NADP^+$, suggesting that a hydrogen bond between the adenosine ribose of NAD^+ and D343, as seen in the X-ray structure of the IMDH binary complex (Dean & Golding, 1997), may have been successfully established in the halophilic enzyme purified from *E. coli*. Thus, we have obtained an ICDH mutant with clearly changed coenzyme specificity (Rodriguez-Arnedo et al., 2005).

Isocitrate specificity changed with the first mutation, but in this case, specificity for isocitrate increased 3- to 10-fold with increasing mutations, suggesting that these mutations favored substrate binding. The maximum value for isocitrate binding occurred when the mutant showed specificity for NAD^+ only. Thus, the mutations markedly influenced not only the K_m for $NAD(P)^+$, but also the K_m for isocitrate. The effect of the mutation on the efficiency for $NADP^+$ or NAD^+ was evaluated by incorporating the K_m for the substrate. This parameter is called the overall catalytic efficiency and is defined as: $(K_{cat}/(K_m{}^{IC} \times K_m{}^{NAD(P)})$ (Table 5) (Nishiyama et al., 1993). We speculate that some specific interaction between the substrate and $NADP^+$, which differs from the native substrate–coenzyme complex, is responsible for the decrease in activity. The ratio K_{cat}/K_m is a measure of both enzyme efficiency and the degree to which an enzyme stabilizes the transition state (Dean & Golding, 1997).

Residues at	NADP+			NAD+		
291 343 344 350 390	K_m (μM)	K_{cat} (min^{-1})	$K_{cat}/K_m \times 10^3$ ($min^{-1}/\mu M$)	K_m (μM)	K_{cat} (min^{-1})	$K_{cat}/K_m \times 10^3$ ($min^{-1}/\mu M$)
R K Y V Y	101±30	0.176±0.020	1.7±0.7	____	_____	_____
S - - - -	350±30	0.244±0.020	0.70±0.12	____	_____	_____
S - - - P	327±50	0.060±0.004	0.18±0.04	____	_____	_____
S D - - P	203±30	0.145±0.008	0.70±0.14	____	_____	_____
S D I - P	282±20	0.020±0.003	0.071±0.016	____	_____	_____
S D I A P	____	_____	_____	144±60	0.0422± 0.0017	0.29±0.13

Residues at	Isocitrate			
291 343 344 350 390	K_m (μM)	K_{cat} (min^{-1})	$K_{cat}/K_m \times 10^3$ ($min^{-1}/\mu M$)	$K_{cat}/(K_m{}^{IC} \times K_m{}^{NAD(P)})$
R K Y V Y	108±30	0.139±0.010	1.3±0.5	1.3×10^{-5}
S - - - -	18±3	0.123±0.002	6.8±1.2	2.0×10^{-5}
S - - - P	36±4	0.032±0.003	0.88±0.18	2.7×10^{-6}
S D - - P	36±5	0.086±0.003	2.4±0.4	1.2×10^{-5}
S D I - P	40±7	0.0149±0.0003	0.37±0.07	1.3×10^{-6}
S D I A P	11±1*	0.0327±0.0013	3.0±0.4*	$2.0 \times 10^{-5*}$

Initial rates were measured spectrophotometrically at 30 °C in 20 mM Tris-HCl buffer pH 8.0, 1 mM EDTA and 10 mM $MgCl_2$ ($Tris/EDTA/Mg^{2+}$) containing 2 M NaCl. Substrate and coenzyme concentrations were varied between 0.019 and 0.10 mM for D,L-isocitrate and between 0.044 and 0.4 mM for $NADP^+$ or NAD^+. Single-letter amino acid codes denote amino acid residues. Catalytic efficiency was measured as K_{cat}/K_m. Asterisks indicate values that were obtained with NAD^+ as the coenzyme. Abbreviations: K_m = Michaelis constant; K_{cat} = turnover number; K_{cat}/K_m = catalytic efficiency; and $K_{cat}/(K_m{}^{IC} \times K_m{}^{NAD(P)})$ = overall catalytic efficiency.

Table 5. Kinetic parameters of purified wild-type and mutant *Hfx. volcanii Ds-threo*-isocitrate dehydrogenases (ICDHs) toward $NADP^+$ and NAD^+.

One might think that a local conformational change induced by specific binding of $NADP^+$ or NAD^+ is responsible for the variation in the behavior of the *Hfx. volcanii* enzyme versus isocitrate. This effect is probably due to less repulsion of the charges in the active site.

The comparison of the sequence with that of the *T. thermophilus* IMDH (Imada et al., 1991) reveals a consistent framework in the evolution of the substrate specificity of the decarboxylating dehydrogenases belonging to the class of isocitrate dehydrogenases. All residues (R117, R127, R151, Y158 and K228) interact with the α- and β-carboxylates and α-hydroxyls of isocitrate, which are common with isopropylmalate and malate; all residues are conserved in all known ICDHs and IMDHs. Two aspartic acid residues, D282 and D306, coordinate Mg^{2+}. They are also conserved in all available sequences. Residues that interact with the γ-carboxylate of isocitrate, S111 and N113 (*Hfx. volcanii* ICDH numbering), are only found in ICDH sequences and are not found in IMDH sequences. Common features of ICDH and IMDH are due to conserved residues that interact with the α- and β-groups and the metal ion. Difference in the substrate specificity is determined by non-conserved residues that interact with the γ-group (Hurley et al., 1991).

4. Conclusion

Site–directed mutagenesis has allowed us to (1) extend the understanding of the molecular basis of salt tolerance for halophilic adaptation, (2) analyze the role of sequence differences between thermophilic and halophilic dehydrogenases involving a ligand to the zinc ion, and (3) identify the residues implicated in coenzyme specificity.

The replacement of aspartic residues by lysine residues on the GlcDH surface have led to a modification of the halophilic properties of the mutant enzymes, D172K and D216K being the most significant mutations (Esclapez et al., 2007).

The mutation of D38, a residue that lies close to the catalytic zinc ion, to C38 or A38 led to a significant reduction in and abolition of activity, respectively. These results suggest that this residue is important in catalysis, either in forming a key aspect of the zinc-binding site or in some other process related with substrate recognition. The replacement of D38 by C38 results in the production of a less efficient enzyme with lower enzymatic activity and catalytic efficiency. Furthermore, this mutant shows slightly more thermostability. Although the D38C GlcDH is less active, it has been crystallized in the presence of several combinations of products and substrates. This fact has allowed us to describe many aspects of the mechanism of the zinc-dependent MDR superfamily (Esclapez et al., 2005; Baker et al., 2009).

Structural analysis of the GlcDH from *Hfx. mediterranei* revealed that the adenosine 2'-phosphate of $NADP^+$ is stabilized by the side chains of R207 and R208. The first attempt to change coenzyme specificity involved making the G206D mutant. Further substitutions of uncharged residues for these residues were made to analyze their importance in $NADP^+$ binding and to improve specificity for NAD^+. The single mutants G206D and R207I were less efficient with $NADP^+$ than the wild type, and the double and triple mutants, G206D/R207I and G206D/R207I/R208N, showed no activity with $NADP^+$ (Pire et al., 2009).

The results obtained in our study with the halophilic ICDH and the complete switch of coenzyme specificities in IMDH from *T. thermophilus* (Imada et al., 1991) and ICDHs from *E. coli* show that coenzyme specificity in the β-decarboxylating dehydrogenases are principally determined by interactions between the nucleotides and surface amino acid residues lining the binding pockets (Rodriguez-Arnedo et al., 2005).

5. Acknowledgment

We thank Dr. Rice, Dr. Baker and Dr. Britton, from The University of Sheffield (UK), for helping us to prepare GlcDH structure figures. This work was supported by Grants from Ministerio de Educación (BIO2002-03179 and BIO2005-08991-C02-01).

6. References

Bonete, M. J., Pire, C., Llorca, F. I. & Camacho, M. L. (1996) Glucose dehydrogenase from the halophilic Archaeon *Haloferax mediterranei*: enzyme purification, characterisation and N-terminal sequence. *FEBS Lett.*, 383: 227-229.

Bradford, M. M. (1976) A rapid and sensitive method for the quantitation of microgram quantities of protein utilizing the principle of protein-dye binding. *Anal. Biochem.*, 72: 248-254.

Baker, P. J., Britton, K. L., Fisher, M., Esclapez, J., Pire, C., Bonete, M. J., Ferrer, J. & Rice, D. W. (2009) Active site dynamics in the zinc-dependent medium chain alcohol dehydrogenase superfamily. *Proc. Natl. Acad. Sci. USA,* 106: 779-784.

Bocanegra, J. A., Scrutton, N. S. & Perham, R. N. (1993) Creation of an NADP-dependent pyruvate dehydrogenase multienzyme complex by protein engineering. *Biochemistry*, 32: 2737–2740.

Britton, K. L., Stillman, T. J., Yip, K. S. P., Forterre, P., Engel, P. C. & Rice, D. W. (1998) Insights into the molecular basis of salt tolerance from the study of glutamate dehydrogenase from *Halobacterium salinarum*. *J. Biol. Chem*., 273: 9023-9030.

Britton, K. L., Baker, P. J., Fisher, M., Ruzheinikov, S., Gilmour, D. J., Bonete, M. J., Ferrer, J., Pire, C., Esclapez, J. & Rice, D. W. (2006) Analysis of protein solvent interactions in glucose dehydrogenase from the extreme halophile *Haloferax mediterranei*. *Proc. Natl. Acad. Sci. USA,* 103: 4846-4851.

Camacho, M. L., Brown, R. A., Bonete, M.-J., Danson, M. J. & Hough, D. W. (1995) Isocitrate dehydrogenases from *Haloferax volcanii* and *Sulfolobus solfataricus:* enzyme purification, characterisation and N-terminal sequence. *FEMS Microbiol. Lett.*, 134: 85-90.

Camacho, M. L., Rodríguez-Arnedo, A. & Bonete, M. J. (2002) NADP-dependent isocitrate dehydrogenase from the halophilic archaeon *Haloferax volcanii*: cloning, sequence determination and overexpression in *Escherichia coli*. *FEMS Microbiol. Lett.*, 209: 155-160.

Chen, R., Greer, A. & Dean, A. M. (1995) A highly active decarboxylating dehydrogenase with rationally inverted coenzyme specificity. *Proc. Natl. Acad. Sci. USA,* 92: 11666–11670.

Chen, R., Greer, A. & Dean, A. M. (1996) Redesigning secondary structure to invert coenzyme specificity in isopropylmalate dehydrogenase. *Proc. Natl. Acad. Sci. USA*, 93: 12171–12176.

Chen, R., Greer, A. & Dean, A. M. (1997) Structural constraints in protein engineering: the coenzyme specificity of *Escherichia coli* isocitrate dehydrogenase. *Eur. J. Biochem*., 250: 578–582.

Dean, A. M. & Golding, G. B. (1997) Protein engineering reveals ancient adaptive replacements in isocitrate dehydrogenase. *Proc. Natl. Acad. Sci. USA,* 94: 3104–3109.

Eisenberg, H., Mevarech, M. & Zaccai, G. (1992) Biochemical, structural and molecular genetic aspects of halophilism. *Adv. Protein Chem*., 43: 1-62.

Eklund, H., Samma, J. P., Wallen, L., Brändén, C. L., Akeson, A. & Jones, T. A. (1981) Structure of a triclinic ternary complex of horse liver alcohol dehydrogenase at 2,9 Å resolution. *J. Mol. Biol*., 146: 561-587.

Esclapez, J., Britton, K. L., Baker, P. J., Fisher, M., Pire, C., Ferrer, J., Bonete, M. J. & Rice, D. W. (2005) Crystallization and preliminary X-ray analysis of binary and ternary complexes of *Haloferax mediterranei* glucose dehydrogenase. *Acta Cryst. F,* 61: 743-746.

Esclapez, J., Pire, C., Bautista, V., Martínez-Espinosa, R. M., Ferrer, J. & Bonete, M. J. (2007) Analysis of acidic surface of *Haloferax mediterranei* glucose dehydrogenase by site-directed mutagenesis. *FEBS Lett.,* 581: 837-842.

Fan, F. & Plapp, B. V. (1999) Probing the affinity and specificity of yeast alcohol dehydrogenase I for coenzymes. *Arch. Biochem. Biophys.,* 367: 240-249.

Ferrer, J., Fisher, M., Burke, J., Sedelnikova, S. E., Baker, P. J., Gilmour, D. J., Bonete, M. J., Pire, C., Esclapez, J. & Rice, D. W. (2001) Crystallization and preliminary X-ray analysis of glucose dehydrogenase from *Haloferax mediterranei*. *Acta Cryst. D,* 57: 1887-1889.

Gómez-Moreno, C. & Sancho, J. (Eds) (2003). *Estructura de Proteínas,* Ariel Ciencia, ISBN 9788434480612, Barcelona, Spain.

Hurley, J. H., Dean, L. A. M., Koshland, Jr., D. E. & Stroud, R. M. (1991) Catalytic Mechanism of $NADP^+$-Dependent Isocitrate Dehydrogenase: Implications from the Structures of Magnesium-Isocitrate and $NADP^+$ Complexes. *Biochemistry*, 30: 8671-8678.

Hurley, J. H. & Dean, A. M. (1994) Structure of 3-isopropylmalate dehydrogenase in complex with NAD^+: ligand induced loop closing and mechanism for cofactor specificity. *Structure,* 2: 1007–1016.

Hurley, J. H., Chen, R. & Dean, A. M. (1996) Determinants of Cofactor Specificity in Isocitrate Dehydrogenase: Structure of an Engineered $NADP^+ \rightarrow NAD^+$ Specificity-Reversal Mutant. *Biochemistry*, 35: 5670–5678.

Imada, K., Sato, M., Tanaka, N., Katsube, Y., Matsuura, Y. & Oshima, T. (1991) Three-dimensional structure of a highly thermostable enzyme, 3-isopropylmalate dehydrogenase of *Thermus thermophilus* at 2.2 Å resolution *J. Mol. Biol.,* 222: 725–738.

Irimia, A., Ebe, C., Madern, D., Richard, S. B., Cosenza, L. W., Zaccai, G. & Vellieux, F. M. D. (2003) The oligomeric states of *Haloarcula marismortui* malate dehydrogenase are modulated by solvent components as shown by crystallographic and biochemical studies. *J. Mol. Biol.,* 326: 859-873.

Jolley, K. A., Rusell, R. J. M., Hough, D. H. & Danson, M. J. (1997) Site-directed mutagenesis and halophilicity of dihydrolipoamide dehydrogenase from the halophilic archaeon, *Haloferax volcanii*. *Eur. J. Biochem.,* 248: 362-368.

Kauri, T., Wallace, R. & Kushner, D. J. (1990) Nutrition of the halophilic archaebacterium, *Haloferax volcanii*. *Syst. Appl. Microbiol.,* 13: 14–18.

Kay, J. & Weitzman, P. D. J. (Eds.) (1987) Krebs' Citric Acid Cycle: Half a Century and Still Turning. *Biochem. Soc. Symp*., 54: l-198.

Lanyi, J. K. (1974) Salt-dependent properties of proteins from extremely halophilic bacteria. *Bacteriol. Rev*., 38: 272-290.

Lloyd, A. J. & Weitzman, P. D. J. (1988) Purification and characterization of NAD-linked isocitrate dehydrogenase from *Methylophilus methylotrophus. Biochem. Soc. Trans*., 16: 871–872.

Madern, D., Pfister, C. & Zaccai, G. (1995) Mutation at a single acidic amino acid enhances the halophilic behavior of malate dehydrogenase from *Haloarcula marismortui* in physiological salts. *Eur. J. Biochem.,* 230: 1088-1095.

Madern, D., Ebel, C. & Zaccai, G. (2000) Halophilic adaptation of enzymes. *Extremophiles*, 4: 91-98.

Madern, D., Camacho, M., Rodríguez-Arnedo, A., Bonete, M.-J. & Zaccai, G. (2004) Salt-dependent studies of NADP-dependent isocitrate dehydrogenase from the halophilic archaeon *Haloferax volcanii*. *Extremophiles*, 8: 377-384.

Nishiyama, M., Birktoft, J. J. & Beppu, T. (1993) Alteration of Coenzyme Specificity of Malate Dehydrogenase from *Thermus flavus* by Site-directed Mutagenesis. *J. Biol. Chem*., 268: 4656–4660.

Pire, C., Camacho, M. L., Ferrer, J., Hough, D. W. & Bonete, M. J. (2000) NAD(P)+- glucose dehydrogenase from *Haloferax mediterranei*: kinetic mechanism and metal content. *J. Mol. Catal. B: Enzym*., 10: 409-417.

Pire, C., Esclapez, J., Ferrer, J. & Bonete, M. J. (2001) Heterologous overexpression of glucose dehydrogenase from the halophilic archaeon *Haloferax mediterranei*, an enzyme of the medium chain dehydrogenase/reductase family. *FEMS Lett*., 200: 221-227.

Pire, C., Esclapez, J., Díaz, S., Pérez-Pomares, F., Ferrer, J. & Bonete, M. J. (2009) Alteration of coenzyme specificity in halophilic NAD(P)$^+$ glucose dehydrogenase by site-directed mutagenesis. *J. Mol. Catal. B: Enzym.,* 59: 261-265

Richard, S. B., Madern, D., Garcin, E. & Zaccai, G. (2000) Halophilic adaptation: novel solvent-protein interactions observed in the 2.9 and 2.6 Å resolution structures of the wild type and a mutant of malate dehydrogenase from *Haloarcula marismortui. Biochemistry,* 39: 992-1000.

Rodríguez-Arnedo, A., Camacho, M. & Bonete, M. J. (2005) Complete reversal of coenzyme specificity of isocitrate dehydrogenase from *Haloferax volcanii*. *Protein J.*, 24: 259-266.

Rodríguez Valera, F., Juez, G. & Kushner, D. J. (1983) *Halobacterium mediterranei* spec. nov., a new carbohydrate utilizing extreme halophile. *System. Appl. Microbiol*., 4: 369-381.

Rosell, A., Valencia, E., Ochoa, W. F., Fita, I, Parés, J. & Farrés, X. (2003) Complete reversal of coenzyme specificity by concerted mutation of three consecutive residues in alcohol dehydrogenase. *J. Biol. Chem*., 278: 40573-40580.

Rossmann, M. G., Moras, D. & Olsen, K. W. (1974) Chemical and biological evolution of nucleotide-binding protein. *Nature,* 250: 194-199.

Serrano, J. A., Camacho, M. & Bonete, M. J. (1998). Operation of glyoxylate cycle in halophilic archaea: presence of malate synthase and isocitrate lyase in *Haloferax volcanii*. *FEBS Lett*., 434: 13–16.

Singh, S. K., Matsuno, K., LaPorte, D. C. & Banaszak, L. J. (2001) Crystal Structure of *Bacillus subtilis* Isocitrate Dehydrogenase at 1.55 Å. Insights Into The Nature of Substrate Specificity Exhibited by *Escherichia coli* Isocitrate Dehydrogenase Kinase/Phosphatase. *J. Biol. Chem*., 276: 26154–26163.

Steen, I. H., Lien, T. & Birkeland, N.-K. (1997) Biochemical and phylogenetic characterization of isocitrate dehydrogenase from a hyperthermophilic archaeon, *Archaeoglobus fulgidus*. *Arch. Microbiol*., 168: 412–420.

Steen, I. H., Lien, T., Madsen, M. S. & Birkeland, N.-K. (2002) Identification of cofactor discrimination sites in NAD-isocitrate dehydrogenase from *Pyrococcus furiosus*. *Arch. Microbiol*., 178: 297–300.

Thompson, J. D., Higgins, D. G. & Gibson, T. J. (1994) CLUSTAL W: improving the sensitivity of progressive multiple sequence alignment through sequence weighting, positions-specific gap penalties and weight matrix choice. *Nucleic Acids Res.,* 22: 4673-4680.

Watanabe, S., Kodaki, T. & Makino, S. (2005) Complete reversal of coenzyme specificity of xylitol dehydrogenase and increase of thermostability by the introduction of structural zinc. *J. Biol. Chem*., 280: 10340-10349.

Yasutake, Y., Watanabe, S., Yao, M., Takada, Y., Fukunaga, N. & Tanaka, I. (2003) Crystal Structure of the Monomeric Isocitrate Dehydrogenase in the Presence of NADP$^+$. Insight into the cofactor recognition, catalysis, and evolution. *J. Biol. Chem*., 278: 36897–36904.